coatings

MDPI

Article

Colloidal Aqueous Dispersions of Methyl (Meth)Acrylate-Grafted Polyvinyl Alcohol Designed for Thin Film Applications

Silvia Bozhilova [1], Katerina Lazarova [2], Sijka Ivanova [1], Daniela Karashanova [2], Tsvetanka Babeva [2,*] and Darinka Christova [1,*]

[1] Institute of Polymers, Bulgarian Academy of Sciences, Akad. G. Bonchev Str., Bl. 103-A, 1113 Sofia, Bulgaria
[2] Institute of Optical Materials and Technologies "Acad. J. Malinowski", Bulgarian Academy of Sciences, Akad. G. Bonchev Str., Bl. 109, 1113 Sofia, Bulgaria
* Correspondence: babeva@iomt.bas.bg (T.B.); dchristo@polymer.bas.bg (D.C.)

Abstract: In this paper, the aqueous copolymer dispersions of methyl (meth)acrylate-grafted poly(vinyl alcohol) are in situ synthesized and studied as a promising platform for the deposition of thin films with advanced applications. A series of dispersions of the varied copolymer structure and composition are obtained at mild reaction conditions by carrying out a redox polymerization at a different monomer-to-PVA ratio and initiator concentration. The obtained colloidal particles are characterized by Fourier transformed infrared spectroscopy, nuclear magnetic resonance, dynamic light scattering, and transmission electron microscopy. The copolymer dispersions are further used for deposition of thin films on silicon substrates. The films are characterized optically through reflectance measurements and non-linear curve fitting. Their suitability for the optical sensing of acetone vapors is confirmed by reflectance measurements before and during their exposure to analyte vapors. The cross sensitivity, sensing repeatability, and recovery of the sensitive films are discussed.

Keywords: polymer colloids; polymer thin films; optical constants; optical sensing

Citation: Bozhilova, S.; Lazarova, K.; Ivanova, S.; Karashanova, D.; Babeva, T. Colloidal Aqueous Dispersions of Methyl (Meth)Acrylate-Grafted Polyvinyl Alcohol Designed for Thin Film Applications. *Coatings* **2022**, *12*, 1882. https://doi.org/10.3390/coatings12121882

Academic Editor: Torsten Brezesinski

Received: 15 November 2022
Accepted: 30 November 2022
Published: 3 December 2022

1. Introduction

Polymer colloids are attractive materials with versatile properties and multiple innovative applications. Their use in various industrial and academic research and development fields ranging from biomedical applications such as medical diagnostics and therapeutics, cosmetics, and personal care to coatings, adhesives, energy storage, etc., is increasingly growing. Nowadays, progress in the area is enabled by the fundamentals of emulsion polymerization and new developments with regard to the particle morphologies, functionality, and emerging applications [1–3]. Special attention is focused on the environmentally friendly waterborne colloidal polymer particles that are able to meet the increasing demands for green and sustainable coatings, especially those based on vinyl chemistries [4,5].

Colloidal dispersions are basic systems for self-assemble nanomaterials (photonic crystals for example) and for the deposition of advanced thin films on a solid substrate [6,7]. Along with the simple drying of a spread thin layer of the suspension on a nonporous substrate, other more controlled approaches such as spin-coating [8] and electrospray are applied for thin film deposition [9].

Acetone is one of the organic solvents widely used as a reaction and/or separation media in various technological processes in chemical and pharmaceutical industries. As it is considered to be harmful to human health, the development of reliable sensors for acetone vapor detection is of vital importance. Acetone is also among the key volatile

organic compounds in the exhaled human breath, resulting from the body's metabolic processes. It is well known that the diabetes patients produce higher amounts of ketones such as acetone. Hence, the rapid and easy detection of the presence of its vapors in the breath, especially when done in a non-invasive way, will be of great value for the early detection and control of diabetes. The existing non-invasive strategies use analytical techniques such as gas chromatography and mass spectrometry, as well as electrochemical sensors and devices of the "electronic nose" type. However, the complexity of the methods and complications of the daily monitoring are definitely not advantageous. To overcome those challenges, optical sensors or biosensors [10] can be used, as in which case a change in the optical or physical property (the thickness, refractive index, reflectance, luminescence, etc.), due to interaction between the analyte of interest and the sensing element, is easily measured [11–16]. As the detection of acetone vapors can be achieved using multiple devices and materials [17–21], finding the most suitable media for creating a fully optical and electrical power-free sensor is of great importance.

Polymers are materials of interest when developing a gas sensor as the efficiency at room temperature is the most important advantage of polymer-based gas sensors. Most often, these sensors are of a conductive type and polymers such as polythiophene, polypyrrole, polyaniline, and their derivatives are usually used as a sensing media [20]. One benefit of the polymer materials is the possibility to improve the sensing properties through developing hybrid materials or composites, by using a chemical functionalization, nanostructuring, etc. [22–24]. So, an easy optical detection can be achieved via a thin film polymer-based sensor that changes its color/reflectance in the presence of acetone vapors, without the need for an electrical power supply and operating at room temperature. To achieve this goal, a copolymer is needed that is sensitive towards acetone and easy to deposit in a layered form.

In this paper we design and synthesize amphiphilic graft copolymers comprising poly(vinyl alcohol) (PVA) main chain and polyacrylate side chains suitable for thin film applications. PVA was chosen as a hydrophilic water-soluble polymer well known for its remarkable mechanical and physical properties, excellent film-forming ability, and good adhesion to a variety of surfaces. As a hydrophobic constituent, two acrylic polymers were selected, namely poly(methyl acrylate) (PMA) and poly(methyl methacrylate) (PMMA) which properties differ significantly. A grafting reaction took place in an aqueous solution and the film-forming properties of the in situ generated copolymer aqueous dispersions were evaluated.

The aqueous dispersions of poly(vinyl alcohol-*g*-methyl acrylate) (PVA-*g*-MA) of a different copolymer composition were tested as environmentally relevant materials for the preparation of thin films with acetone-sensing properties. The copolymer dispersions were deposited on silicon substrates by the spin-coating method. The optical as well as sensing properties of the studied thin copolymers films were investigated and the changes in the reflectance ΔR, thickness Δd, and refractive index Δn in the presence of acetone vapors were followed.

2. Materials and Methods

2.1. Materials

Poly(vinyl alcohol) (PVA, approx. Mw 9000–10,000, 80% hydrolyzed, CAS 9002-89-5), methyl acrylate (MA, 99%, CAS 96-33-3), methyl methacrylate (MMA, 99%, CAS 80-62-6), ammonium cerium(IV) nitrate (CAN, ≥98.5%, CAS 16774-21-3), and nitric acid (HNO_3, 70%, CAS 7697-37-2) were purchased from Sigma-Aldrich (Saint Louis, MO, USA) MA and MMA were passed through a column of activated basic alumina and purged with nitrogen prior to use.

2.2. Synthesis of Copolymer Aqueous Dispersions

The copolymer aqueous dispersions used in this work were synthesized by grafting MA and MMA on PVA as initiating hydroxyl moiety. The redox polymerization in deionized water was applied using ammonium cerium(IV) nitrate as the initiator according to the procedures described in the literature [25,26], adapted to the present system. In brief, a dilute PVA solution was prepared and bubbled with nitrogen for 15 min for the removal of the oxygen. The solution was cooled down to 10 °C and then the initiator solution in 1 N HNO_3 was added under vigorous stirring followed by the chosen amount of comonomer (MA or MMA, respectively). The reaction mixture was bubbled with nitrogen for another 15 min and transferred to a bath thermostated at 35 °C. The polymerization was implemented for 3 h at 35 °C under a nitrogen atmosphere. As a result, water-soluble PVA chains were converted to water-insoluble graft macromolecules self-assembled in particulate nanostructures due to the aqueous media. The colloidal aqueous dispersions obtained in situ were purified by dialysis against deionized water and used for a thin film deposition after adjusting the concentration. A portion of any dispersion was freeze dried and the isolated polymer was used for the copolymer characterization.

2.3. Methods

2.3.1. Fourier Transformed Infrared Spectroscopy

The Fourier transform infrared (FTIR) spectra were recorded using an IRAffinity-1 spectrophotometer (Shimadzu Company, Kyoto, Japan) equipped with an MIRacleTM ATR accessory (diamond crystal; PIKE Technologies, Madison, WI, USA) providing the depth of penetration of the IR beam into the sample of about 2 μm. All the samples were scanned over the wave number range from 4000 to 600 cm^{-1} performing 50 scans at a resolution of 4 cm^{-1}.

2.3.2. Nuclear Magnetic Resonance

The NMR analyses were performed on a Bruker Avance II+ 600 NMR spectrometer (Billerica, MA, USA). The proton spectra were measured in deuterated dimethyl sulfoxide (DMSO-d6). The copolymer compositions were estimated based on the integrated proton NMR spectra when comparing the integrals of the signals of the PVA and PMA or PMMA repeating units.

2.3.3. Dynamic Light Scattering

The particle size and dispersity of the copolymer dispersions were studied by dynamic light scattering (DLS) using a NanoBrook Plus PALS instrument (Brookhaven Instruments, Holtsville, NY, USA) equipped with a 35 mW solid-state laser operating at λ = 660 nm at a scattering angle of 90°. The particles' hydrodynamic diameters (D_H) were determined according to the Stokes–Einstein equation:

$$D_H = kT/(3\pi\eta D) \quad (1)$$

where k is the Boltzmann's constant, T is the absolute temperature, η is the viscosity of the solution, and D is the diffusion coefficient. The measurements were carried out in an automated mode in triplicate and recorded as the average value of 3 runs. The standard deviations of the measurement (STD) along with D_H are used for the calculation of the dispersity (DI):

$$DI = (STD/D_H)^2 \quad (2)$$

2.3.4. Transmission Electron Microscopy

The morphology of the copolymer particles was studied by transmission electron microscopy (TEM) using a high-resolution transmission electron microscope JEOL JEM 2100 (JEOL Ltd., Tokyo, Japan). The preliminary preparation of the samples consisted of

the dropping and drying of the dispersions on a standard TEM copper grids covered by an amorphous carbon layer. All the analyses were performed at an accelerating voltage of 200 kV.

2.3.5. Differential Scanning Calorimetry

Differential scanning calorimetry (DSC) analyses were carried out on Perkin–Elmer DSC 8500 (PerkinElmer, Inc., Waltham, MA, USA) equipment. The samples were analyzed in the temperature range from −20 °C to 200 °C at a scanning rate of 10 °C/min.

2.3.6. Thin Film Deposition and Optical Characterization Methods

Thin films of CP2 and CP4 were deposited by a spin-coating method (WS-650-23 B, Laurel, MS, USA) using 0.200 mL of the copolymer aqueous solution on pre-cleaned Si substrates and at a rotation rate of 4000 rpm for 60 s. After the deposition, the polymer films were annealed in air at 60 °C for 30 min. The reflectance spectra R of the films were measured with an accuracy of 0.3% by a UV–Vis–NIR spectrophotometer (Cary 5E, Varian, Sydney, Australia). The measured reflectance spectra were used for the determination of the thickness (d) and optical constants (refractive index, n and extinction coefficient, k) of the thin films through the non-linear curve-fitting method [27].

2.3.7. Sensing Experiments

In order to perform the sensing experiment and to simulate the presence of acetone and the non-acetone ambient, thin films were placed in a quartz cell, inside of which the atmosphere can be controlled by a homemade bubbler system that generates vapors from liquids [28]. The reflectance spectra of the films were measured in the same spot prior to and during the exposure to the acetone vapors and then the maximum reflectance change ΔR was calculated by using the equation:

$$\Delta R = |R_{ac} - R_{ar}| \quad (3)$$

where R_{ac} and R_{ar} are the reflectance of the films in the ambient of the acetone vapors and argon, respectively. To evaluate the change in the thickness Δd, the refractive index change, Δn, and the swelling degree, SD, induced by the exposure of the films to the acetone vapors, the reflectance spectra measured in the argon and in the acetone vapors were used and the corresponding parameters were calculated as:

$$\Delta d = d_{ac} - d_{ar} \quad (4)$$

$$\Delta n = n_{ac} - n_{ar} \quad (5)$$

$$SD(\%) = 100 * |\Delta d|/d_{ar} \quad (6)$$

where d_{ac} and d_{ar} are the thicknesses of the films in the acetone and argon ambient, respectively, while n_{ac} and n_{ar} are the refractive indices of the films in the respective ambient.

3. Results and Discussion

3.1. In Situ Synthesis of Colloidal Dispersions and Characterization of the Corresponding Amphiphilic Graft Copolymers

PVA-based colloidal dispersions were synthesized at environmentally friendly reaction conditions, namely water as the reaction medium and the relatively low reaction temperature of 35 °C. The series of amphiphilic graft copolymers comprising the PMA (PVA-*g*-PMA) and PMMA (PVA-*g*-PMMA) side chains in a form of colloidal particles dispersed in an aqueous medium were obtained by varying the monomer mole fraction as well as the initiator concentration. The chemical structure of the obtained copolymers is illustrated in Figure 1.

Table 1 summarizes the reaction conditions and characteristics of the obtained copolymers. For the PVA-g-PMA copolymer series, the particle yield is high (over 80%) and independent of the monomer and initiator concentration within the investigated range. The same observation is valid for the particle hydrodynamic diameter D_H and dispersity index. It can be concluded that the redox polymerization of MA onto the low molar mass PVA in a diluted aqueous solution is an advantageous method providing the homogeneous colloidal dispersions of particles in the nanometer size range and narrow size distribution.

On the other hand, when grafting MMA by applying the optimal reaction conditions specified for the PVA-*g*-PMA series (i.e., sample CP4), a coarse and inhomogeneous dispersion is obtained at a lower reaction yield and much larger particle diameter and size distribution (Table 1; sample CP5). The further decrease in the MMA concentration in the reaction mixture does not impart any improvement in the quality of the PVA-*g*-PMMA aqueous dispersion (Table 1; sample CP6). It needs to be mentioned that the values for the D_H of the samples CP5 and CP6, listed in Table 1, are indicative and shown only as an illustration of the dispersion quality.

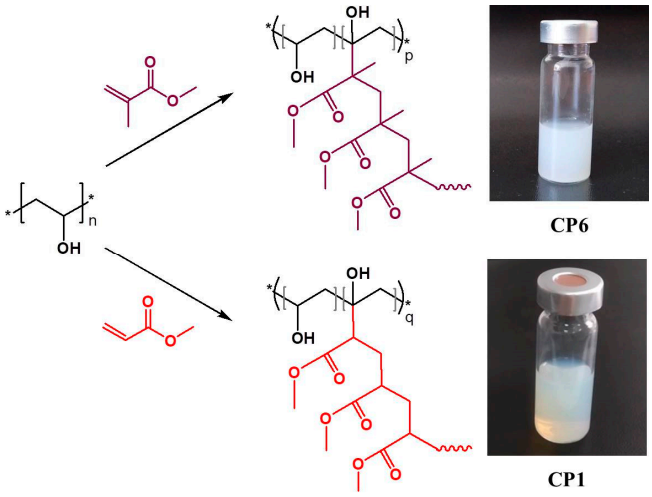

Figure 1. Schematic presentation of the reaction of grafting MA and MMA on PVA.

Table 1. Grafting reaction conditions and characteristics of the obtained colloidal particles.

Sample Code	Reaction Conditions [a]				Yield [%]	Grafted Monomer Mole Fraction in Copolymer Composition [b]	Particle Size and Size Distribution [c]	
	Grafted Monomer	Concentration [mol/L]	Mole Fraction	CAN [mol/L] × 10^3			D_H [nm]	Dispersity
CP1	MA	0.35	0.50	3.0	92.6	0.60	69	0.067
CP2	MA	0.35	0.50	4.5	81.8	0.61	70	0.077
CP3	MA	0.70	0.67	4.5	89.1	0.74	86	0.069
CP4	MA	0.35	0.50	9.0	95.4	0.61	73	0.067
CP5	MMA	0.35	0.50	9.0	75.1	0.52	2693 [d]	0.91 [d]
CP6	MMA	0.18	0.25	9.0	80.3	0.37	6783 [d]	0.86 [d]

(a) [PVA] = 15.0 g/L, 35 °C, 180 min; (b) calculated from 1H NMR spectra; (c) average hydrodynamic diameters and dispersity indexes as measured by DLS at concentration of copolymer aqueous dispersions of 1 g/L; (d) indicative values which are out of the measurement's validated range.

The observed inconsistency in the results from grafting MA and MMA onto PVA in the aqueous media can be explained, bearing in mind the distinctive differences in the properties of PMA and PMMA themselves. PMA is known to be a soft, tough, and rubbery material at room temperature (T_g of about 10 °C), whereas PMMA with a glass transition at approx. 105 °C is a strong, hard, and clear plastic material [29]. Obviously,

the reaction conditions used (more specifically the lower polymerization temperature) favor the homogeneous MA grafting and preparation of uniform colloidal dispersions, whereas smooth MMA grafting is probably complicated resulting in the coarse dispersion of the aggregated particles. Indeed, the DSC analysis of the lyophilized copolymers confirmed these explanations, showing glass transitions of 25.6 °C for CP2 and 15.7 °C for CP4, in contrast with the glass transitions of CP5 and CP6 at around 100 °C and 92 °C, respectively.

The copolymer composition of the obtained colloidal particles was evaluated by using conventional methods including NMR and FTIR. Figure 2 shows the proton NMR spectra of CP1, representative of the PVA-*g*-PMA series, and CP5 exemplary for PVA-*g*-PMMA. The assignment of the characteristic peaks of both copolymer backbones (PVA) and side chains (PMA or PMMA) is shown on the spectra. The copolymer compositions indicated in Table 1 are estimated from the integrated spectra by comparing the integrated area of the peaks at 3.8 ppm assigned to the methine groups of PVA with the integrals of the signals at about 3.6 ppm referring to the methyl functions of the PMA or PMMA segments.

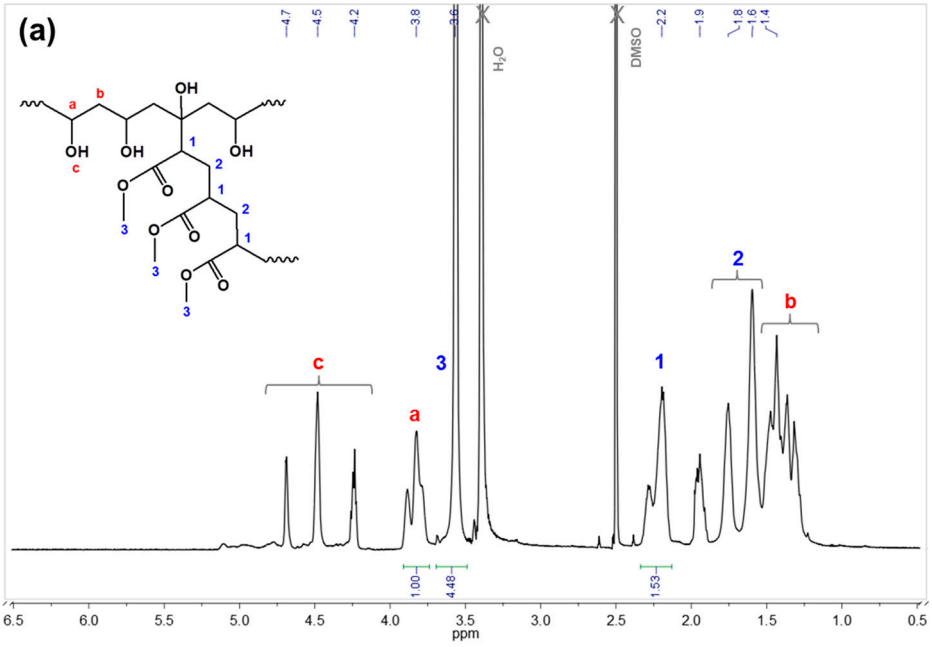

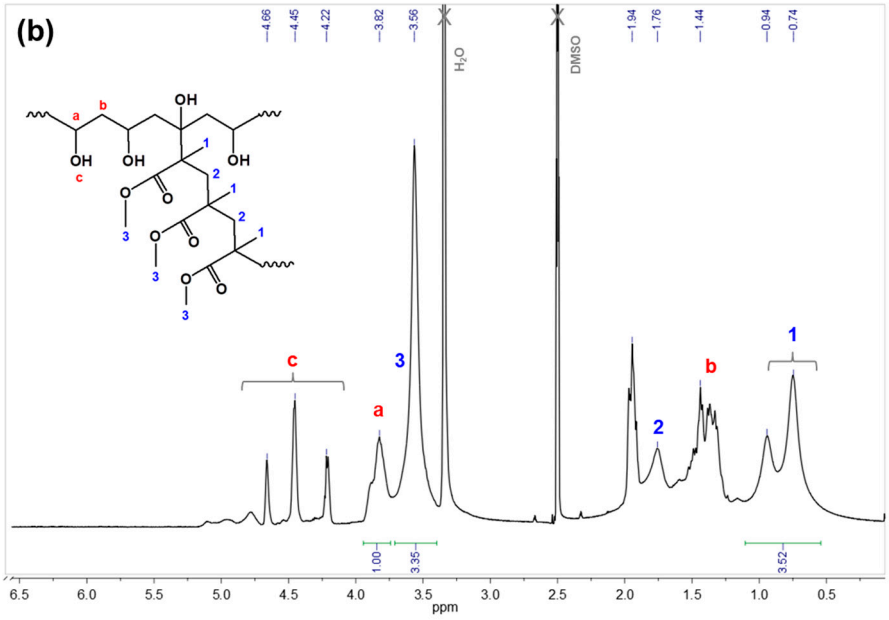

Figure 2. ^{1}H NMR spectra (600 MHz; solvent DMSO-d_6) of (**a**) CP1; and (**b**) CP5.

The copolymer composition was confirmed by the FTIR analysis of the lyophilized colloidal particles. In Figure 3, the FTIR spectrum of the original PVA is compared to those of CP1, and CP5 representative of the PVA-*g*-PMA and PVA-*g*-PMMA series, respectively. In the spectrum of CP1, major absorption bands identified at 1728 cm^{-1} (C=O stretch) and 1161 cm^{-1} (C-O stretch) clearly confirm the carbonyl groups of the PMA present along with the characteristic bands of the PVA backbone. In the spectrum of CP5, the corresponding bands of the PMMA carbonyl groups appear at 1724 cm^{-1} and 1145 cm^{-1}, respectively.

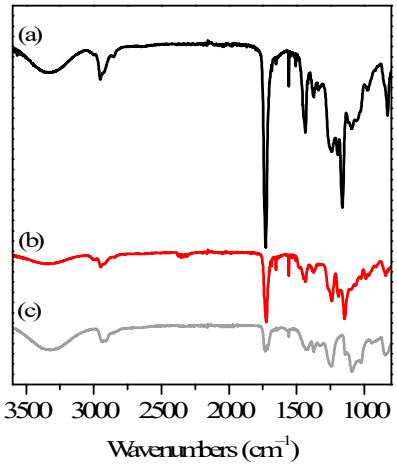

Figure 3. FTIR spectra of (**a**) CP1 and (**b**) CP5 as compared to original PVA (**c**).

3.2. Properties of Obtained Colloidal Aqueous Dispersions

The particles' size and size distribution of the dispersions of the PVA-*g*-PMA series were further investigated by using DLS and visualized via transmission electron microscopy (TEM). Table 2 presents the results from the DLS measurement obtained at the dilution of the original aqueous dispersions of the PVA-*g*-PMA copolymers. As can be seen from the data in Table 1, the prepared dispersions consist of particles with diameters in a close nanometer range (60–80 nm) and a narrow size distribution. The particle pa-

rameters do not change significantly with the two-fold and three-fold dilution, which is indicative for stable colloidal dispersions (Table 2). Moreover, the dispersity, that describes the width of the particle size distribution, is less than or around 0.1, that implies the monodisperse particles distribution.

Table 2. Particle size and size distribution of PVA-*g*-PMA colloidal aqueous dispersions at different copolymer concentrations.

Sample Code	Mole Fraction of MA	Concentration [g/L]	D_H [nm]	Dispersity
CP1	0.60	5.0	70	0.043
		1.0	69	0.067
		0.5	66	0.086
CP2	0.61	5.0	71	0.103
		1.0	70	0.077
		0.5	68	0.109
CP3	0.74	5.0	82	0.117
		1.0	86	0.069
		0.5	83	0.075
CP4	0.61	5.0	72	0.101
		1.0	73	0.067
		0.5	66	0.132

The TEM micrographs of the two dispersions of the PVA-g-PMA series, namely CP2 and CP4, are shown in Figure 4. CP2 and CP4 are identical DLS parameters (Table 2) and differ only in the copolymer structure: CP4 is obtained by a two-fold increase in the initiator concentration (Table 1), which implies a much higher grafting density compared to CP2. The TEM images in Figure 4 clearly show the formation of particles with a spherical shape for both the CP2 and CP4 copolymers. It can be seen also that the morphology of the CP2 and CP4 particles is complex and consists of a core and shell, visualized on the TEM images with their different electronic contrast. The particles of the two copolymers differ by their inner structure due to the differences in the polymeric chains. For CP2, the formation of a single core symmetrically located in the central zone of the particle is typical, while in CP4, the dispersion multicore particles were produced predominantly.

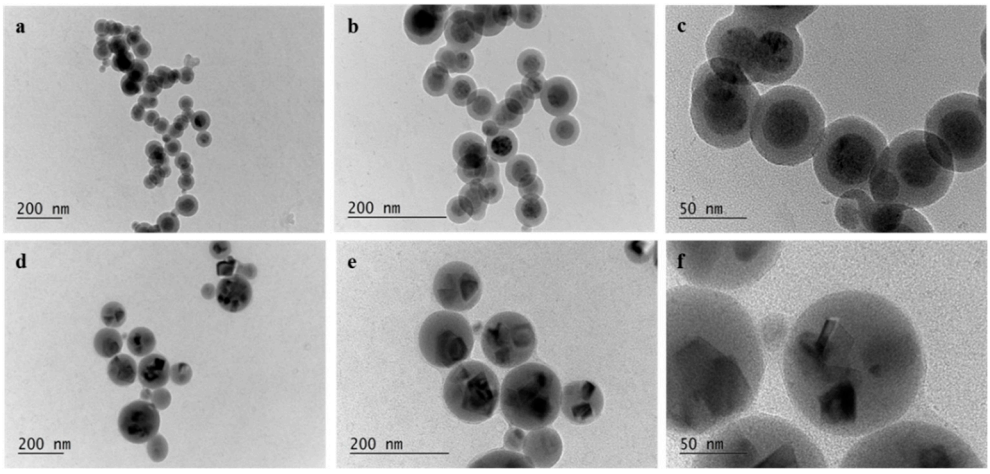

Figure 4. Bright Field TEM micrographs of CP2 (**a**–**c**) and CP4 (**d**–**f**) at different magnifications (20,000× (**a**,**d**), 40,000× (**b**,**e**), and 100,000× (**c**,**f**)).

3.3. Thin Films of PVA-g-PMA—Preparation and Optical Characterization

Copolymers with a middle (CP2) and high (CP4) grafting density were selected to be prepared as thin films with an approximate thickness of 70 nm. Purposely, the same

concentrations of the colloidal aqueous dispersions of CP2 and CP4 were prepared and spin-coated on silicon substrates. The films are transparent, free of cracks, and have a smooth surface, which is confirmed by the examination of the surface topography and roughness through a 3D optical profiler. The reflectance spectra of the polymer films were measured at a normal light incidence in the spectral range 320–800 nm and are presented in Figure 5 along with a picture of the CP2 sample as an inset to represent the typical color of both coatings. It can be seen in Figure 5 that the difference in the reflectance spectra of the two polymer films is very small, as could be expected considering the same colors of the films. Generally, on the basis of the measured spectra, a conclusion of a similar thickness and optical constants could be drawn. To confirm this, the optical constants (refractive index, n and extinction coefficient, k) and thickness, d, were calculated by a two-stage non-linear curve-fitting method [27] that minimizes the discrepancies between the measured and calculated R-curves. The values of n, k, and d are presented in Table 3.

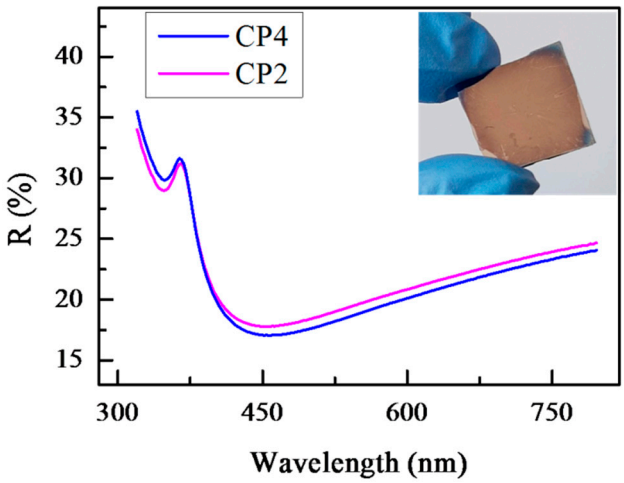

Figure 5. Reflectance spectra of CP2 and CP4 copolymer thin films and picture of CP2 film on silicon substrate as an inset.

Table 3. Thickness, d, refractive index, n, extinction coefficient, k of CP2 and CP4 copolymer films, reflectance change ($\Delta R = |R_{ac} - R_{ar}|$), thickness of the film exposed to acetone vapors, d_{ac}, swelling degree, SD = $(d_{ac} - d_{ar})/d_{ar}$, and refractive index change $\Delta n = n_{ac} - n_{ar}$ after exposure to acetone vapors.

Sample	d (nm)	n at 600 nm	k at 600 nm	ΔR (%)	d_{ac} (nm)	SD (%)	Δn
CP2	71	1.34	0.018	3.5	77.6	9.3	−0.01
CP4	73	1.35	0.017	6	83.6	14.5	−0.01

It can be seen from Table 3 that the refractive index, extinction coefficient, and thickness of both copolymer films are very similar. This means that the grafting density has a weak impact on the films' optical properties and thickness. However, it should be noted that the n-values of 1.34 and 1.35 of the copolymer films are lower compared to the refractive indices of PMA and PVA that both have n-values of 1.48 at a wavelength of 600 nm [29,30]. Considering that the films' density is related to the refractive index, we could conclude that the copolymer films have a lower density as compared to PVA and PMA. The possible explanation is that the globular structure and the grafting of the copolymers are responsible for the generation of a free volume in the films that results in a low density and refractive index, respectively. Moreover, it is seen from Table 3 that the refractive index of the CP2 films is slightly lower compared to the n-value of the CP4 films. The possible reason is the lower grafting density of the CP2 polymer, resulting in the lower overall density of the film.

3.4. Sensing Properties

If a polymer film is sensitive to any external stimuli, it will change its thickness and/or/ refractive index when in contact, which will consequently change its reflectance spectra and color. In our case, in order to study the optical properties and swelling behavior of thin polymer films in the presence and absence of acetone vapors, the films are placed in a quartz cell with parallel transparent walls and the ambient inside the cell is cycled from the argon to acetone vapors and the reflectance spectra of the film are measured without moving the sample, thus ensuring that the same spot on the sample for all the measurements is probed and the observed difference in the measured spectra correlates only with change in the optical parameters and thickness of the films [31].

The reflectance spectra for the CP4 film measured in argon and acetone vapors are presented in Figure 6a, while the difference between the spectra at a wavelength of 342 nm is presented in Figure 6b. The value of 342 nm is selected as the wavelength at which ΔR has the highest value.

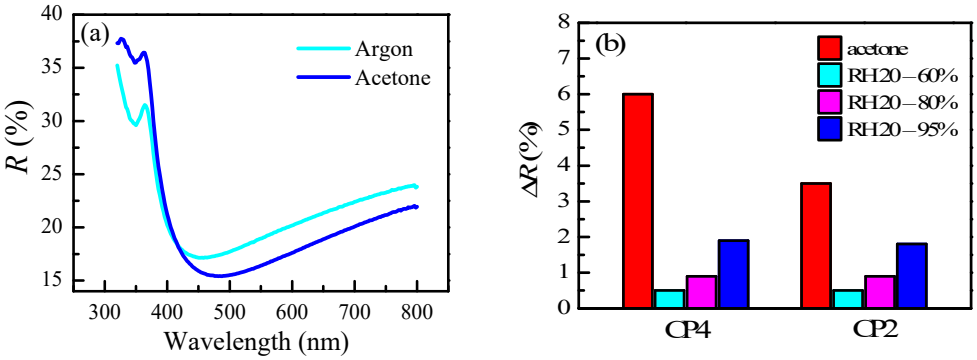

Figure 6. Reflectance spectra of CP4 copolymer thin films measured in ambient of argon and acetone vapors (**a**) and reflectance change ΔR for CP2 and CP4 thin film samples due to acetone exposure (red bars) and due to relative humidity exposure in the ranges 20%–60% (cyan bars), 20%–80% (magenta bars), and 20%–95% (blue bars) (**b**).

It is seen that after the exposure to acetone vapors, the spectrum minimum located at a wavelength of 450 nm is redshifted with 26 nm. The change in the reflectance ΔR at a wavelength of 342 nm reaches the maximum values of 6% for CP4 and 3.5% for the CP2 films.

The measured spectra in argon and acetone are further used for the calculation of the refractive index and thickness of the films. The changes in the refractive index and the thickness (Δn and swelling degree, SD, respectively) are calculated and presented in Table 3. When exposed to the acetone vapors, both films exhibit a swelling mostly pronounced in the CP4 film (14.5%) where the thickness increases from 73 nm to 83.6 nm. For comparison, the CP2 film swells by 9.3%, i.e., its thickness changes from 71 nm to 77.6 nm. The probable reason for the higher sensitivity observed for the CP4 film is its higher grafting density as compared to CP2, that leads to a stronger swelling. As shown in Table 3, the swelling is accompanied with a small decrease in the refractive index Δn = 0.01 which is the same for both films.

In order to study the humidity cross sensitivity, the polymer films were exposed to different levels of relative humidity (RH) and the reflectance values were measured at each RH. Figure 6b presents the change in the reflectance of the films when the humidity varies in three different ranges: 20%–60%, 20%–80%, and 20%–95%. It is seen that the influence of the humidity in the typical working conditions of a sensor (20%–60% RH) is negligible; the reflectance change is 0.5%. Moreover, should a sensor operate in a very high humidity, for example 95%, the sensitivity to acetone would be 3 times higher than the one to humidity.

In order to test the reversibility of the copolymer films' sensing properties, the reflectance at 342 nm is monitored in time over 3 cycles of the absorption and desorption of acetone. The results are depicted in Figure 7. After introducing the acetone vapors, the film starts to swell, leading to an increase in the measured reflectance signal. When the acetone is switched off, a fast desorption takes place, accompanied with a decrease in film thickness. A recovery of the initial signal is observed within less than 5 min without an additional annealing. A similar behavior is observed for the next cycles and there is no difference in the level of steady state signal reached. This means that the thickness change in the copolymer films is reversible and there is no need of an additional annealing for the recovery. Moreover, the swelling and shrinkage of the films is reproducible.

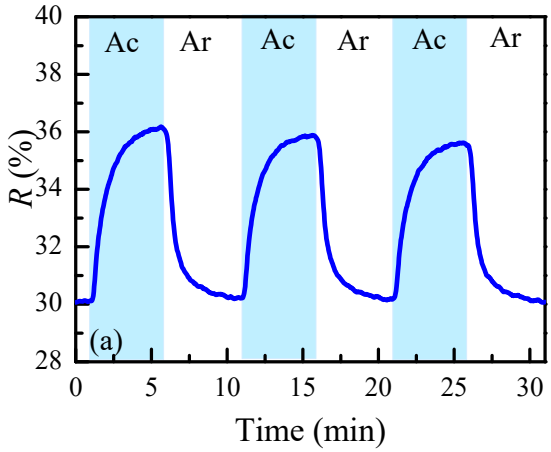

Figure 7. Reflectance measured at a wavelength of 342 nm for copolymer film CP4 within 3 cycles of absorption and desorption of acetone vapors.

4. Conclusions

The successful preparation of the aqueous colloidal systems of amphiphilic PVA-copolymers with grafted methyl acrylate and methyl methacrylate side chains suitable for the direct deposition of thin polymer films was demonstrated. It was found that varying the monomer and the initiator concentration when grafting MA onto PVA did not significantly affect the size of the colloidal particles; the hydrodynamic diameters remained in the interval of 70–80 nanometers with an almost constant size dispersity. However, when grafting MMA onto PVA, coarse and inhomogeneous dispersions were obtained which were deemed to not be suitable for a thin film deposition.

Transparent and cracks-free thin films with an approximate thickness of 70 nm were prepared by the spin-coating of colloidal dispersions of MA grafted PVA with two different grafting densities. The optical characterization revealed that the grafting density has a weak influence on the optical properties and thickness of the films. When exposed to acetone vapors, thin films exhibit a swelling mostly pronounced in the films with a higher grafting density. Additional adsorption/desorption cycling measurements prove that the thickness change in the copolymer films is reversible and that there is no need for an additional annealing for their recovery.

Author Contributions: Conceptualization, T.B. and D.C.; methodology, T.B., D.C. and K.L.; software, T.B. and K.L.; validation, S.B., T.B., D.C. and K.L.; formal analysis, S.B., T.B., D.C., D.K. and K.L; investigation, K.L., S.B., S.I. and D.K.; resources, D.C. and T.B.; data curation, K.L., S.B., S.I., D.C. and T.B.; writing—original draft preparation, K.L., T.B. and D.C.; writing—review and editing, T.B., D.C. and K.L.; visualization, K.L., T.B. and D.C.; supervision, T.B. and D.C.; project administration, T.B. and D.C. All authors have read and agreed to the published version of the manuscript.

Funding: This research received partial funding from CoE "National center of mechatronics and clean technologies" BG05M2OP001-1.001-0008-C01 supported by the European Regional Devel-

opment Fund within the Operational Programme "Science and Education for Smart Growth 2014–2020" and from Bulgarian National Science Fund under the grant agreement no. KII-06-H47/1/26.11.2020.

Institutional Review Board Statement: Not applicable.

Informed Consent Statement: Not applicable.

Data Availability Statement: Not applicable.

Acknowledgments: Research equipment of Distributed Research Infrastructure INFRAMAT, part of Bulgarian National Roadmap for Research Infrastructures, supported by Bulgarian Ministry of Education and Science was used in this investigation.

Conflicts of Interest: The authors declare no conflict of interest.

References

1. Priestley, R.D.; Prud'homme, R.K. *Polymer Colloids: Formation, Characterization and Applications*; Soft Matter Series No. 9. The Royal Society of Chemistry: Croydon, UK, 2020.
2. Lovell, P.A.; Schork. F.J. Fundamentals of Emulsion Polymerization. *Biomacromolecules* **2020**, *21*, 4396−4441.
3. Sundberg, D. Structured, Composite Nanoparticles from Emulsion Polymerization—Morphological Possibilities. *Biomacromolecules* **2020**, *21*, 4388–4395.
4. Klier, J.; Bohling, J.; Keefe, M. Evolution of functional polymer colloids for coatings and other applications. *AIChE J.* **2016**, *62*, 2238–2247.
5. Anastas, P.T.; Warner, J.C. *Green Chemistry: Theory and Practice*; Oxford University Press: New York, NY, USA, 1998.
6. Wasan, D.; Nikolov, A.; Moudgil, B. Colloidal dispersions: Structure, stability and geometric confinement. *Powder Technol.* **2005**, *153*, 135–141.
7. Xu, P.; Mujumdar, A.S.; Yu, B. Drying-Induced Cracks in Thin Film Fabricated from Colloidal Dispersions. *Dry. Technol.* **2009**, *27*, 636–652.
8. Larson, R.G.; Rehg, T.J. Spin Coating. *Liquid Film Coating*; Springer: Dordrecht, The Netherlands, 1997.
9. Rahman, K.; Phung, T.H.; Oh, S.; Kim, S.H.; Ng, T.N.; Kwon, K.-S. High-Efficiency Electrospray Deposition Method for Non-conductive Substrates: Applications of Superhydrophobic Coatings. *ACS Appl. Mater. Interfaces* **2021**, *13*, 18227–18236.
10. Usman, F.; Dennis, J.; Ahmed, A.; Meriaudeau, F.; Ayodele, O.; Rabih, A. A Review of Biosensors for Non-Invasive Diabetes Monitoring and Screening in Human Exhaled Breath. *IEEE Access* **2019**, *7*, 5963–5974.
11. Thévenot, D.; Toth, K.; Durst, R.; Wilson, G. Electrochemical biosensors: Recommended definitions and classification. *Pure Appl. Chem.* **1999**, *71*, 2333–2348.
12. Dey, D.; Goswami, T. Optical biosensors: A revolution towards quantum nanoscale electronics device fabrication. *J Biomed. Biotechnol.* **2011**, 348218.
13. Ünlü, M.; Chiari, M.; Özcan, A. Introduction to the special issue of optical biosensors. *Nanophotonics* **2017**, *6*, 623–625.
14. Borisov, S.; Wolfbeis, O. Optical Biosensors. *Chem. Rev.* **2008**, *108*, 423–461.
15. Sun, Y.-S.; Landry, J.; Zhu, X. Evaluation of Kinetics Using Label-Free Optical Biosensors. *Instrum. Sci. Technol.* **2017**, *45*, 486–505.
16. Ligler, F.; Taitt, C. *Optical Biosensors: Present & Future*; Gulf Professional Publishing: Houston, TX, USA, 2002.
17. Righettoni, M.; Tricoli, A. Toward portable breath acetone analysis for diabetes detection. *J. Breath Res.* **2011**, *5*, 037109.
18. Bhowmik, B.; Manjuladevi, V.; Gupta, R.K.; Bhattacharyya, P. Highly Selective Low-Temperature Acetone Sensor Based on Hierarchical 3-D TiO_2 Nanoflowers. *IEEE Sens. J.* **2016**, *16*, 3488–3495.
19. Nooke, A. *Gas Detection by Means of Surface Plasmon Resonance Enhanced Ellipsometry*; Federal Institute for Materials Research and Testing, BAM: Berlin, Germany, 2012.
20. Lakard, B.; Carquigny, S.; Segut, O.; Patois, T.; Lakard, S. Gas Sensors Based on Electrodeposited Polymers. *Metals* **2015**, *5*, 1371–1386.
21. Karthikeyan, S.; Pandya, H.; Sharma, M.; Gopal, K. Gas Sensors—A Review. *J. Environ. Nanotechnol.* **2015**, *4*, 1–14.
22. Oueiny, C.; Berlioz, S.; Perrin, F. Carbon nanotube-polyaniline composites. *Prog. Polym. Sci.* **2014**, *39*, 707–748.
23. Marini, M.; Pilati, F.; Pourabbas, B. Smooth Surface Polypyrrole-Silica Core-Shell Nanoparticles: Preparation, Characterization and Properties. *Macromol. Chem.* **2008**, *209*, 1374–1380.
24. Chithra Iekha, P.; Subramanian, E.; Padiyan, D. Electrodeposition of polyaniline thin films doped with dodeca tungstophosphoric acid: Effect on annealing and vapor sensing. *Sens. Actuators B* **2007**, *122*, 274–281.
25. Chowdhurya, P.; Pal, C.M. Graft copolymerization of methyl acrylate onto polyvinyl alcohol using Ce(IV) initiator. *Eur. Polym. J.* **1999**, *35*, 2207–2213.
26. Lazarova, K.; Vasileva, M.; Ivanova, S.; Novakov, C.; Christova, D.; Babeva, T. Influence of Macromolecular Architecture on the Optical and Humidity-Sensing Properties of Poly(*N*,*N*-Dimethylacrylamide)-Based Block Copolymers. *Polymers* **2018**, *10*, 769.

27. Lazarova, K.; Vasileva, M.; Marinov, G.; Babeva, T. Optical characterization of sol–gel derived Nb_2O_5 thin films. *Opt. Laser Technol*. **2014**, *58*, 114–118.
28. Lazarova, K.; Awala, H.; Thomas, S.; Vasileva, M.; Mintova, S.; Babeva, T. Vapor Responsive One-Dimensional Photonic Crystals from Zeolite Nanoparticles and Metal Oxide Films for Optical Sensing. *Sensors* **2014**, *14*, 12207–12218.
29. Corsaro, C.; Neri, G.; Santoro, A.; Fazio, E. Acrylate and Methacrylate Polymers' Applications: Second Life with Inexpensive and Sustainable Recycling Approaches. *Materials* **2022**, *15*, 282.
30. Bodurov, I.; Vlaeva, I.; Viraneva, A.; Yovcheva, T.; Sainov, S. Modified design of a laser refractometer. *Nanosci. Nanotechnol.* **2016**, *16*, 31–33.
31. Lazarova, K.; Bozhilova, S.; Ivanova, S.; Christova, D.; Babeva, T. Optical Characterization of Acetone-Sensitive Thin Films of poly(vinyl alcohol)-g-poly(methyl acrylate). *Chem. Proc.* **2021**, *5*, 41.